ORGANIC LETTERS

2009
Vol. 11, No. 4
795−798

A Zn^{2+} Fluorescent Sensor Derived from 2-(Pyridin-2-yl)benzoimidazole with Ratiometric Sensing Potential

Zhipeng Liu,[†] Changli Zhang,[†,§] Yunling Li,[†] Zhengyi Wu,[†] Fang Qian,[†] Xiaoliang Yang,[†] Weijiang He,[*,†] Xiang Gao,[‡] and Zijian Guo[*,†]

State Key Laboratory of Coordination Chemistry, Coordination Chemsitry Institute, School of Chemistry and Chemical Engineering, Nanjing Universitry, Nanjing 210093, P. R. China, Animal Model Research Center, Nanjing University, Nanjing 210061, P. R. China, and Department of Chemistry, Nanjing Xiaozhuang College, Nanjing 210017, P. R. China

zguo@nju.edu.cn; heweij69@nju.edu.cn

Received November 19, 2008

ABSTRACT

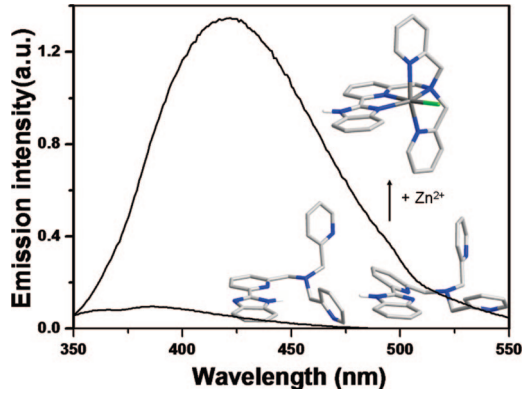

A fluorescent Zn^{2+} sensor based on the 2-(2′-pyridinyl)benzoimidazole (2-PBI) fluorophore has been devised by incorporation with a Zn^{2+} ionophore, bis(pyridin-2-ylmethyl)amine. The sensor (PBITA) demonstrates a Zn^{2+}-specific emission shift and enhancement with a 1:1 binding ratio. Due to the Zn^{2+}-induced coplanation of 2-PBI via reversion/rotation, PBITA is shown to behave as a ratiometric sensor. The intracellular Zn^{2+} imaging ability of the sensor has been tested in HeLa cells using a confocal microscope.

As the second most abundant transition-metal ion in the human body, Zn^{2+} is actively involved in various biological processes.[1] Spatiotemporal determination of Zn^{2+} in biological samples utilizing fluorescent sensors is of great significance for understanding the role of Zn^{2+} in biology. As a consequence, development of novel fluorescent sensors for Zn^{2+} has received considerable current attention.[2−8] Most of the currently reported Zn^{2+} fluorescent sensors have the nature of metal chelation enhanced fluorescence (MCHEF),[9] which functions via Zn^{2+} binding-induced emission enhancement. Normally, the quantum yield of fluoresent sensors displays distinct environment-dependence. This property

[†] Coordination Chemsitry Institute.
[‡] Animal Model Research Center.
[§] Nanjing Xiaozhuang College.

(1) Berg, J. M.; Shi, Y. *Science* **1996**, *271*, 1081–1085.
(2) Kimura, E.; Kioke, T. *Chem. Soc. Rev.* **1998**, *27*, 179–184.
(3) Burdette, S. C.; Lippard, S. L. *Proc. Natl. Acad. Sci. U.S.A.* **2003**, *100*, 3605–3610.
(4) Kikuchi, K.; Komatsu, H.; Nagano, T. *Curr. Opin. Chem. Biol.* **2004**, *8*, 182–191.
(5) Jiang, P.; Guo, Z. *Coord. Chem. Rev.* **2004**, *248*, 205–229.
(6) Thompson, R. B. *Curr. Opin. Chem. Biol.* **2005**, *9*, 526–532.
(7) Carol, P.; Sreejith, S.; Ajayaghosh, A. *Chem. Asian J.* **2007**, *2*, 338–348.

10.1021/ol802537c CCC: $40.75
Published on Web 01/21/2009

allows these MCHEF sensors to visualize the change of Zn^{2+} concentration, but they cannot provide quantified information about $[Zn^{2+}]_{free}$. Ratiometric Zn^{2+} sensors are capable of overcoming this problem because Zn^{2+} binding to them induces shift in excitation or emission maxima, and internal calibration can be achieved by measuring the ratio of apo-sensor and Zn^{2+}-bound sensor. Then, not only the environment-dependence but also the artifacts caused by the variations in excitation intensity, emission collection efficiency, and photobleaching can be largely reduced by internal calibration. However, ratiometric fluorescent Zn^{2+} sensors suitable for practical intracellular Zn^{2+} imaging are rare so far,[10] due to the scarcity of suitable fluorophore prototypes displaying zinc chelation-induced emission/excitation shift.[10,11] Therefore, there is a huge scope and potential for exploring novel fluorophores for ratiometric Zn^{2+} sensing.

A common fluorophore, 2-(2′-pyridinyl)benzoimidazole (2-PBI), is widely used in coordination chemistry for its ability to bind an array of *d*- and *f*-block elements. It is able to act as both fluorophore and ionophore for Zn^{2+} and displays a specific emission shift in both aqueous and acetonitrile solution owing to Zn^{2+}-chelation via 2, 2′-N atoms. However, 2-PBI fails to qualify as a ratiometric Zn^{2+} sensor due to the low Zn^{2+} binding affinity and variable Zn^{2+} binding modes.[12] Increasing the Zn^{2+} coordination number of 2-PBI could enhance the Zn^{2+} binding ability and define the Zn^{2+} binding mode, which will be favorable for the construction of practical Zn^{2+} ratiometric sensors.

Herein, a fluorescent sensor derived from the 2-PBI platform, PBITA, was prepared. In this compound, the Zn^{2+} chelator bis(pyridin-2-ylmethyl)amine (BPA) moiety was incorporated with 2-PBI at its 3′-position as the synergic Zn^{2+} coordination motif of its 2,2′-N atoms. Then, both 1:1 Zn^{2+} binding mode and higher Zn^{2+} binding affinity were expected. The synthetic procedure of PBITA is depicted in Scheme 1. A refluxing ethanol solution containing *o*-phenylenediamine and 6-(hydroxymethyl)pyridine-2-carbaldehyde in the presence of $NaHSO_3$ afforded compound **1**, and PBITA was obtained with satisfactory yield by reacting the tosylated derivative of **1** with BPA in CH_3CN in the presence of K_2CO_3 (Supporting Information).

Scheme 1. Synthesis of PBITA

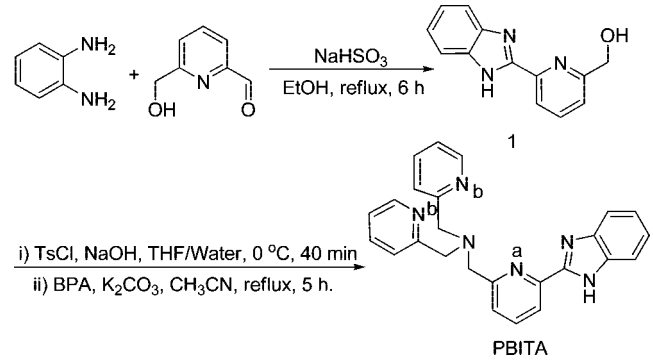

The metal-binding behavior of PBITA has been determined by UV−vis and fluorescence spectroscopic studies. Although PBITA is not highly water soluble, it can be dissolved in water when 10% (v/v) of DMSO was added and all the following studies were carried out in aqueous solution containing 10% DMSO. This protocol is commonly used in many reported Zn^{2+} sensors for intracellular Zn^{2+} imaging.[9h−j,10b] The UV−vis spectrum of PBITA in HEPES buffer exhibits a maximal absorption band centered at 312 nm ($\varepsilon = 9.2 \times 10^4\ M^{-1}\ cm^{-1}$) with a shoulder band at 327 nm (Figure S4, Supporting Information). When titrated by Zn^{2+} (0 − 2 equiv), the intensity of the maximal absorption band decreased with the concomitant increase of the shoulder band. The presence of a clear isobestic point implies the conversion of free PBITA sensor to the only Zn^{2+} complex. The titration profile can be drawn from the absorbance changes at 312 nm, which suggests a 1:1 Zn^{2+} binding mode of PBITA. The stoichiometry of the Zn^{2+}/PBITA complex has also been confirmed by mass spectroscopic determination. The electrospray ionization mass spectrum of this complex displays two signals of *m*/*z* 235.16 and 469.25, which can be assigned as the signals for $[M + Zn - H]^+$ and $[M + Zn]^{2+}$, respectively. The ^1H NMR data provided further evidence for the 1:1 binding ratio (Figure S7, Supporting Information). All the aromatic and alkyl protons of PBITA showed evident chemical shift changes in the titration experiment, suggesting the involvement of 2,2′-N atoms of 2-PBI and all the N atoms of the BPA motif in Zn^{2+} coordination.

Free PBITA in neutral HEPES buffer (DMSO/water = 1:9, v/v) exhibits weak fluorescence with two emission bands

(8) Berg, J. M.; Shi, Y.; Que, E. L.; Domaille, D. W.; Chang, C. J. *Chem. Rev.* **2008**, *108*, 1517–1549.

(9) (a) Komatsu, K.; Kikuchi, K.; Kojima, H.; Urano, Y.; Nagano, T. *J. Am. Chem. Soc.* **2005**, *127*, 10197–10204. (b) Chang, C. J.; Nolan, E. M.; Jaworski, J.; Burdette, S. C.; Sheng, M.; Lippard, S. J. *Chem. Biol.* **2004**, *11*, 203–210. (c) Nolan, E. M.; Ryu, J. W.; Jaworski, J.; Feazell, R. P.; Sheng, M.; Lippard, S. J. *J. Am. Chem. Soc.* **2006**, *128*, 15517–15528. (d) Tang, B.; Huang, H.; Xu, K. H.; Tong, L. L.; Yang, G. W.; Liu, X.; An, L. G. *Chem. Commun.* **2006**, 3609–3611. (e) Gong, H.-Y.; Zheng, Q.-Y.; Zhang, X.-H.; Wang, D.-X.; Wang, M.-X. *Org. Lett.* **2006**, *8*, 4895–4898. (f) Liu, Y.; Zhang, N.; Chen, Y.; Wang, L.-H. *Org. Lett.* **2007**, *9*, 315–318. (g) Wang, H.-H.; Gan, Q.; Wang, X.-J.; Xue, L.; Liu, S.-H.; Jiang, H. *Org. Lett.* **2007**, *9*, 4995–4998. (h) Nasir, M. S.; Fahrni, C. J.; Suhy, D. A.; Kolodsick, K. J.; Singer, C. P.; O'Halloran, T. V. *J. Biol. Inorg. Chem.* **1999**, *4*, 775–783. (i) Fahrni, C. J.; O'Halloran, T. V. *J. Am. Chem. Soc.* **1999**, *121*, 11448–11458. (j) Jiang, P.; Chen, L.; Lin, J.; Liu, Q.; Ding, J.; Gao, X.; Guo, Z. *Chem. Commun.* **2002**, 1424–1425.

(10) (a) Maruyama, S.; Kikuchi, K.; Hirano, T.; Urano, Y.; Nagano, T. *J. Am. Chem. Soc.* **2002**, *124*, 10650–10651. (b) Taki, M.; Wolford, J. L.; O'Halloran, T. V. *J. Am. Chem. Soc.* **2004**, *126*, 712–713. (c) Chang, C. J.; Jaworski, J.; Nolan, E. M.; Sheng, M.; Lippard, S. J. *Proc. Natl. Acad. Sci. U.S.A.* **2004**, *101*, 1129–1134.

(11) (a) Woodroofe, C. C.; Lippard, S. J. *J. Am. Chem. Soc.* **2003**, *125*, 11458–11459. (b) Henary, M. M.; Wu, Y.; Fahrni, C. J. *Chem.—Eur. J.* **2004**, *10*, 3015–3025. (c) Lim, N. C.; Schuster, J. V.; Porto, M. C.; Tanudra, M. A.; Yao, L. L.; Freake, H. C.; Bruckner, C. *Inorg. Chem.* **2005**, *44*, 2018–2030. (d) Ajayaghosh, A.; Carol, P.; Sreejith, S. *J. Am. Chem. Soc.* **2005**, *127*, 14962–14963. (e) Mei, Y. J.; Bentley, P. A. *Bioorg. Med. Chem. Lett.* **2006**, *16*, 3131–3134. (f) Huang, S.; Clark, R. J.; Zhu, L. *Org. Lett.* **2007**, *9*, 4999–5002. (g) Komatsu, K.; Urano, Y.; Kojima, H.; Nagano, T. *J. Am. Chem. Soc.* **2007**, *129*, 13447–13454. (h) Zhang, Y.; Guo, X.; Si, W.; Jia, L.; Qian, X. *Org. Lett.* **2008**, *10*, 473–476.

(12) (a) Wang, C.; Li, Z.; Du, C.; Wang, P. *J. Coord. Chem.* **2008**, *61*, 760–767. (b) Haneda, S.; Gan, Z.; Eda, K.; Hayashi, M. *Organomet.* **2007**, *26*, 6551–6555. (c) Si, Z.; Li, J.; Li, B.; Zhao, F.; Liu, S.; Li, W. *Inorg. Chem.* **2007**, *46*, 6155–6163. (d) Liu, Q.-D.; Jia, W.-L.; Wang, S. *Inorg. Chem.* **2005**, *44*, 1332–1343.

centered at 360 and 385 nm, respectively, with λ_{ex} of 336 nm (Figure 1). The conformational change of PBITA (vide infra) should be responsible for the dual emission behavior (Figure 1, bottom spectrum).[13] Its quantum yield in neutral buffer is 0.048 (Supporting Information). The titration of Zn^{2+} into PBITA gave a new emission band centered at 423 nm which showed a linear enhancement with the increase of $[Zn^{2+}]_{total}$ when the ratio of $[Zn^{2+}]_{total}$/[PBITA] is below or equal to 1:1. When the ratio reached 1:1, however, higher $[Zn^{2+}]_{total}$ did not lead to any further emission enhancement. The remarkable bathochromic shift made PBITA a potential ratiometric sensor for Zn^{2+}. The emission band at 360 nm also displayed some minor changes in intensity. When 1.0 molar equiv of Zn^{2+} was added, the ratio of the emission intensity at 423 and 360 nm (F_{423}/F_{360}) increased from 0.77 (free PBITA) to 7.66 (Zn^{2+}/PBITA complex). On the other hand, the pH titration results of PBITA demonstrated that F_{423}/F_{360} varies slightly from 1.3 at pH 6.4 to 1.4 at pH 7.3, which makes it suitable for application in physiological conditions (Figure S8, Supporting Information).

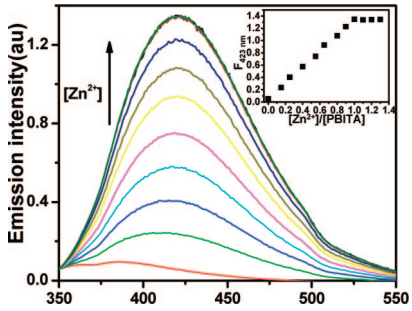

Figure 1. Emission spectra of PBITA (1×10^{-5} M) obtained in HEPES buffer (50 mM, DMSO/water = 1:9, v/v, pH = 7.2) when titrated with Zn^{2+} (1×10^{-2} M). λ_{ex}, 336 nm. The $[Zn]_{total}$ values are 0, 1.5, 2.5, 4.0, 5.5, 6.5, 8.0, 9.0, 10.0, 11.0 μM (from bottom to top). The inset is the corresponding Zn^{2+} titration profile according the emission at 423 nm.

The Zn^{2+}-specific ratiometric response of PBITA was further confirmed by screening the biologically relevant metal cations. As shown in Figure 2, all tested metal cations except Zn^{2+} did not induce any distinct emission shift and enhancement. Moreover, the presence of Na^+, K^+, Ca^{2+}, and Mg^{2+}, which are abundant in cells, did not interfere with the ratiometric response to Zn^{2+}, even though their concentration was 1000 times higher than $[Zn^{2+}]_{total}$. A competitive binding experiment gave an estimated K_d of 7.9×10^{-12} M for Zn^{2+}/PBITA complex (Figure S6, Supporting Information). The quantum yield for the Zn^{2+}/PBITA complex is 0.075. Therefore, PBITA has the favorable property required for intracellular Zn^{2+} imaging.

The intracelluar Zn^{2+} imaging behavior of PBITA on HeLa cells was studied with a laser scanning confocal microscope.

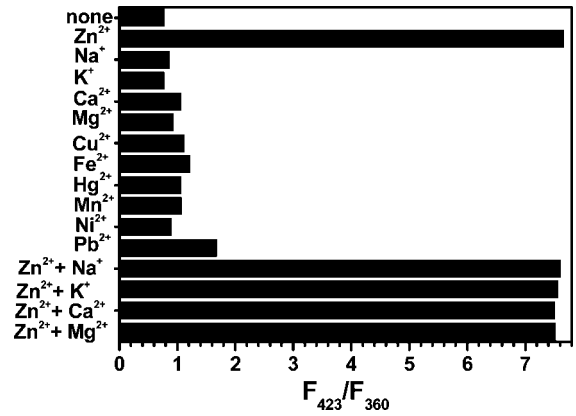

Figure 2. Emission ratio at 423 and 360 nm of PBITA (5 μM) induced by different metal cations in HEPES buffer (50 mM, pH 7.2, 0.1 M KNO_3, DMSO/water = 1:9, v/v). λ_{ex}, 336 nm. The final concentration for Zn^{2+}, Cu^{2+}, Fe^{2+}, Hg^{2+}, Mn^{2+}, Ni^{2+}, and Pb^{2+} is 10 μM, for Na^+, K^+, Ca^{2+}, and Mg^{2+} is 2 mM.

After incubation with PBITA solution (10 μM in PBS, DMSO/water = 1:9, v/v) at 25 °C for 20 min, the HeLa cells displayed very faint intracellular fluorescence (Figure 3). However, HeLa cells exhibited intensive fluorescence when exogenous Zn^{2+} was introduced into the cells via incubation with $ZnSO_4$/pyrithione solution. Moreover, the intensive fluorescence was deeply depressed by scavenging Zn^{2+} from the cells with the cell permeable metal chelator, *N*,*N*,*N*′,*N*′-tetrakis(2-pyridylmethyl)ethylenediamine (TPEN). These results indicate that PBITA is an effective intracellular Zn^{2+} imaging agent with cell permeability. It also implies that 2-(pyridin-2-yl)benzoimidazole could be an effective model fluorophore to construct ratiometric sensors for Zn^{2+}.

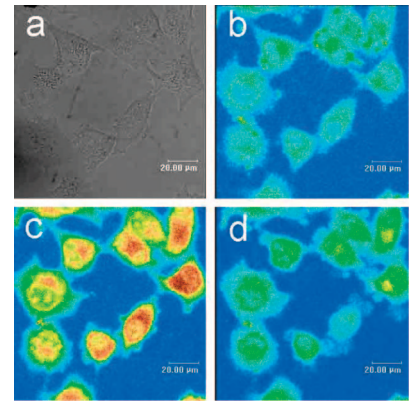

Figure 3. Confocal fluorescence imaging of HeLa cells: (a) bright-field transmission image of cells labeled with PBITA (10 μM, PBS solution containing 10% DMSO) at 25 °C for 20 min; (b) fluorescence image of (a); (c) fluorescence image after incubation with 5 μM $ZnSO_4$/pyrithione (1:1) solution followed by rinse with 10 μM PBITA solution; (d) fluorescence image of HeLa cells in (c) followed by further incubation with 50 μM TPEN solution for 20 min. λ_{ex}, 356 nm. The transformation from light green to brown denotes the emission enhancement. Bar = 20 μm.

(13) (a) Tangoulis, V.; Malamatari, D. A.; Soulti, K.; Stergiou, V.; Raptopoulou, C. P.; Terzis, A.; Kabanos, A.; Kessissoglou, D. P. *Inorg. Chem.* **1996**, *35*, 4974–4983. (b) Dave, B. C.; Czernuszewicz, R. S. *Inorg. Chem. Commun.* **1994**, *227*, 33–41. (c) Battaglia, L. P.; Ferrari, M. F.; Corradi, A. B.; Fave, G. G.; Pelizzi, C.; Tani, M. E. V. *J. Chem. Soc., Dalton Trans.* **1976**, 2197–2202.

The ratiometric sensing behavior of PBITA was further investigated by molecular modeling. Two stable conformations of free PBITA optimized by density functional theory (DFT) calculations at the B3LYP/6-31G(d,p) level (Gaussian 03)[14] are shown in Figure 4. The proton attached to the imidazole N atom locates respectively at the same side of pyridine N*a* in conformation **A** (cis-form) and at the opposite of pyridine N*a* in conformation **B** (trans-form). The dihedral angle between the 2-pyridine plane and benzoimidazole plane is 0° in **A** and 23.34° in **B**, respectively. The two stable forms should be responsible for the dual emission of the sensor. On the other hand, the structure of the Zn^{2+}/PBITA complex (**C**) was also optimized with an initial structure constructed with direct Zn^{2+} coordination by three N atoms of BPA, two 2,2′-N atoms of 2-PBI, and one Cl^{-}. The optimized structure of the Zn^{2+}/PBITA complex displays a dihedral angle of 0.93° between 1,1′-bridged aryl planes. Moreover, the proton attached to the imidazole N atom points to the opposite direction of pyridine N*a*. The theoretical study demonstrates that Zn^{2+}-binding leads to the coplanation of the 1,1′-bridged aryl planes via the reversion or rotation of a benzoimidazole motif from the cis- (A) or trans-form (B). The polarized moment of the PBITA molecule is distinctly changed in the Zn^{2+} binding process, which results in the shift of absorption/emission band. The blockage of the photoinduced electron transfer (PET) process from a BPA amine to a 2-PBI fluorophore induced by Zn^{2+} coordination to a BPA amine should provide for Zn^{2+}-induced emission enhancement.

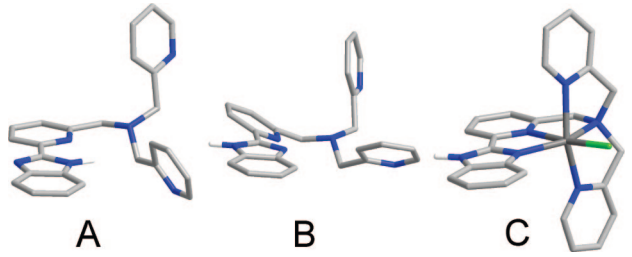

Figure 4. Conformations of PBITA optimized by density functional theory calculations: free PBITA (A, B) and Zn^{2+}/PBITA complex (C). All of the protons except for the one attached to imidazole N atom are omitted for clarity.

In conclusion, a novel Zn^{2+} fluorescent sensor, PBITA, demonstrates a Zn^{2+}-specific ratiometric sensing behavior. The incorporation of a BPA motif provides additional synergic Zn^{2+} coordination sites, which gives exclusively zinc complex with a 1:1 stoichiometry. The intracellular Zn^{2+} imaging ability on HeLa cells demonstrates that PBITA is an effective Zn^{2+} imaging agent. Molecular modeling study suggests that the Zn^{2+}-induced red emission shift of PBITA could be correlated to the coplanation of two heteroaromatic planes of 2-PBI via Zn^{2+}-induced reversion or rotation. Current results indicate that the 2-PBI fluorophore and analogues can be potentially applied for ratiometric Zn^{2+} sensing. Compared with the ratiometric sensors functioning via Zn^{2+} binding induced-deprotonation, such as AQZ,[11h] the ratiometric sensing behavior of the current sensor shows lower relevance to the pK_a value of sensor. The results indicated that 2-PBI provides a valuable framework for the construction of effective Zn^{2+}-specific ratiometric sensors.

Acknowledgment. We thank the National Science Foundation of China (Nos. 20571043, 20631020, 90713001, 20871066, and 20721002) and the Natural Science Foundation of Jiangsu Provence (BK2008015) for financial support. We are grateful to the High Performance Computing Center of Nanjing University for the award of CPU hours to accomplish this work.

Supporting Information Available: Experimental details and characterization of PBITA and selected fluorescence data. This material is available free of charge via the Internet at http://pubs.acs.org.

OL802537C

(14) Firsch, M. J. et al. *Gaussian 03*, Revision D.01; Gaussian, Inc.: Wallingford, CT, 2004. For the full reference, see the Supporting Information.